

Contribution from the Chemical Crystallography Laboratory, University of Oxford, Oxford OX1 3PD, U.K., and Central Research and Development, Experimental Station, E. I. du Pont de Nemours and Co., Inc., Wilmington, Delaware 19898

## Structure of $\text{MnPO}_4 \cdot \text{H}_2\text{O}$ by Synchrotron X-ray Powder Diffraction

Philip Lightfoot,<sup>1</sup> Anthony K. Cheetham,\*<sup>1</sup> and Arthur W. Sleight<sup>2</sup>

Received March 6, 1987

The crystal structure of  $\text{MnPO}_4 \cdot \text{H}_2\text{O}$  has been determined from high-resolution synchrotron X-ray powder diffraction data. The powder pattern was indexed on the basis of 20 accurately measured reflections by an automatic indexing program. Integrated intensities were obtained for 61 unambiguously indexed reflections and used to generate a Patterson map from which the position of the manganese atom was determined. The remaining non-hydrogen atoms were located by Fourier methods, and the hydrogen atom was placed geometrically and refined without constraints. Refinement of the entire diffraction profile, by the Rietveld method, converged to final agreement factors  $R_{wp} = 0.161$ ,  $R_p = 0.122$ , and  $R_1 = 0.047$ . The compound crystallizes in the monoclinic space group,  $C2/c$ , with lattice parameters  $a = 6.912$  (1) Å,  $b = 7.470$  (1) Å,  $c = 7.357$  (1) Å,  $\beta = 112.3$  (1)°, and  $Z = 4$ . The structure consists of axially distorted  $\text{MnO}_6$  octahedra linked together, through the oxygen atom of the water molecule at a common vertex, to form zigzag  $-\text{Mn}-\text{O}-\text{Mn}-$  chains running parallel to  $[101]$ . These chains are interconnected by  $\text{PO}_4$  tetrahedra to form a continuous three-dimensional network.

### Introduction

Both X-ray and neutron powder diffraction data have been used for several years to refine structural models of relatively simple crystal structures, most frequently by Rietveld<sup>3</sup> analysis of the whole diffraction profile.<sup>4</sup> The solution of unknown structures from powder data is, however, a much more serious proposition and has only been achieved in a very few notable cases. Berg and Werner<sup>5</sup> employed Guinier-Hagg film data to solve the structure of  $(\text{NH}_4)_4[(\text{MoO}_2)_4\text{O}_3](\text{C}_4\text{H}_3\text{O}_5)_2 \cdot \text{H}_2\text{O}$  and Clearfield et al.<sup>6</sup> used X-ray powder diffractometer data to solve the structure of  $\text{ZrK}(\text{PO}_4)_2$ . No prior knowledge of the structure was assumed in either case. Recent advances in instrumentation have led to a new generation of very high resolution neutron<sup>7</sup> and X-ray<sup>8</sup> diffractometers. The feasibility of carrying out structural analysis by the Rietveld method using data collected on the new generation of synchrotron X-ray source diffractometers has been demonstrated by Hastings et al.<sup>9</sup> More recently, it has been shown that the quantity of intensity information that can be extracted from these instruments, in terms of nonoverlapping unique reflections, is sufficient to make the routine ab initio solution of simple crystal structures from powder data a feasible prospect. This is illustrated by recent successes with both types of radiation: the solution of the  $\text{FeAsO}_4$  structure<sup>10</sup> by direct methods using high-resolution neutron diffraction data, and that of  $\alpha\text{-CrPO}_4$ <sup>11</sup> by the Patterson method using synchrotron X-ray diffraction data.

This paper presents an example of the use of one of these instruments, the high-resolution powder X-ray diffractometer X13A at the National Synchrotron Light Source, Brookhaven National Laboratory, for the solution and refinement of a previously unknown structure, that of a hydrated manganese phosphate originally assigned the composition  $\text{MnPO}_4 \cdot 1.5\text{H}_2\text{O}$ .<sup>12</sup> The powder X-ray diffraction pattern of this phase was not previously indexed, thus presenting an additional challenge for the technique.

### Experimental Section

**Sample Preparation and Characterization.** A sample of " $\text{MnPO}_4 \cdot 1.5\text{H}_2\text{O}$ " was obtained as a pale green powder by the following method.  $\text{Mn}_3\text{O}_4$  (prepared by the decomposition of manganese(II) oxalate, BDH reagent grade, at 600 °C) was added to a mixture of  $\text{H}_3\text{PO}_4$  (85% in water) and  $\text{H}_2\text{O}$  to produce an approximate 1:10:50 molar ratio of  $\text{Mn}_3\text{O}_4:\text{H}_3\text{PO}_4:\text{H}_2\text{O}$ . This mixture was sealed in a Teflon-lined stainless-steel autoclave and held at 200 °C for 3 days. The product was filtered, washed with cold water, and dried at room temperature. The X-ray powder pattern agreed well with that reported for  $\text{MnPO}_4 \cdot 1.5\text{H}_2\text{O}$  by Goloshchapov et al.<sup>12</sup> X-ray microanalysis of the product, by the "ratio method",<sup>13</sup> in a JEOL 2000FX electron microscope, confirmed a Mn:P ratio of 1, with  $\text{Mn}_2\text{P}_2\text{O}_7$  used as a standard. Thermogravimetric analysis on a Du Pont Instruments 1090B thermal analyzer revealed a continuous weight loss of 15.3% in the range 407–620 °C (Figure 1). The product of this heat treatment, a pale pink powder, gave an X-ray powder pattern corresponding to that of  $\text{Mn}_2\text{P}_2\text{O}_7$ .

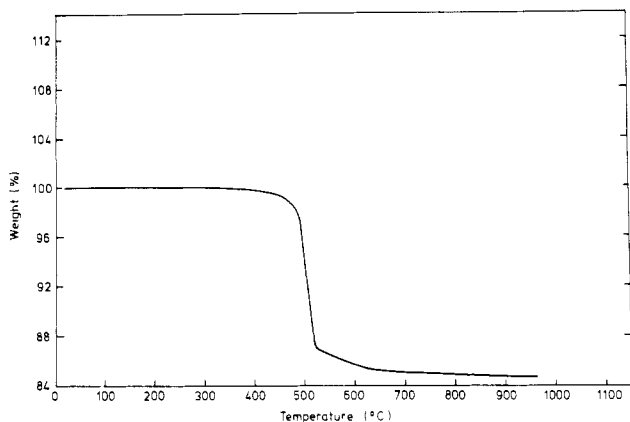
**Data Collection.** Synchrotron X-ray powder data were collected on the X13A beam line at the Brookhaven NSLS. X-rays of wavelength 1.3208 Å were selected by using a perfect Ge(111) crystal monochromator diffracting in the horizontal plane. The sample was placed on a flat plate, and X-rays scattered in the vertical plane were measured via a Ge(200) crystal analyzer and detector. In order to ensure scattering from a sufficiently large number of crystallites and also to reduce any preferred orientation effects, the sample plate was rocked 1 or 2° about the  $\theta$  axis as data collection proceeded. Data were collected in the range  $2\theta = 13\text{--}73^\circ$ , with a step size of 0.005° and counting times of 2–3.5 s/step. A full description of the instrument is given by Cox et al.<sup>8</sup>

**Structure Determination and Refinement.** The powder pattern was indexed on the basis of 20 accurately measured nonoverlapping reflections by using the program of Visser.<sup>14</sup> An  $A$ -centered monoclinic cell of dimensions  $a = 7.361$  Å,  $b = 7.475$  Å,  $c = 6.916$  Å, and  $\beta = 112.32^\circ$  was elucidated from this, giving a "de Wolff figure of merit",<sup>15</sup>  $M_{20} = 196$ . All the observed peaks could be accounted for on the basis of this cell. Transformation of the cell to the conventional  $C$ -centered geometry revealed, in addition to the absences due to  $C$ -centering ( $hkl$ ,  $h + k = 2n + 1$ ), a further absence condition ( $h0l$ ,  $l = 2n + 1$ ), suggesting a  $c$ -glide. The possible space groups were therefore the acentric  $Cc$  (No. 9) or centric  $C2/c$  (No. 15).

Integrated intensities were obtained for 61 unambiguously indexed reflections, several of which were derived from partially overlapping reflections that could be deconvoluted satisfactorily by assuming a "pseudo-Voigt"<sup>16</sup> peak shape. After being corrected for multiplicity and Lorentz effects, the 61  $F_{\text{obsd}}$  values were used to generate a Patterson map. The position of Mn(1) was determined from this, assuming the space group  $C2/c$ , and a series of difference Fourier maps revealed the positions of the phosphorus and three oxygen atoms. The empirical formula thus obtained was " $\text{MnPO}_5$ ". A preliminary  $R$  factor,  $R_F = 13\%$ , based upon the integrated intensities, was obtained after refinement of these atomic positions, which were then used as the starting model for a profile refinement.

- (1) University of Oxford.
- (2) E. I. du Pont de Nemours and Co., Inc.
- (3) Rietveld, H. M. *J. Appl. Crystallogr.* **1969**, *2*, 65.
- (4) Cheetham, A. K.; Taylor, J. C. *J. Solid State Chem.* **1977**, *21*, 253.
- (5) Berg, J.-E.; Werner, P.-E. *Z. Kristallogr., Kristallgeom., Kristallphys., Kristallchem.* **1977**, *145*, 310.
- (6) Clearfield, A.; McCusker, L. B.; Rudolf, P. R. *Inorg. Chem.* **1984**, *23*, 4679.
- (7) Johnston, M. W.; David, W. I. F. *Rutherford Appleton Lab., [Rep.] RL 1985*, RL-85/122.
- (8) Cox, D. E.; Hastings, J. B.; Cardoso, L. P.; Finger, L. W. *Mater. Sci. Forum* **1986**, *9*, 1.
- (9) Hastings, J. B.; Thomlinson, W.; Cox, D. E. *J. Appl. Crystallogr.* **1984**, *17*, 85.
- (10) Cheetham, A. K.; David, W. I. F.; Eddy, M. M.; Jakeman, R. J. B.; Johnston, M. W.; Torardi, C. C. *Nature (London)* **1986**, *320*, 46.
- (11) Atfield, J. P.; Sleight, A. W.; Cheetham, A. K. *Nature (London)* **1986**, *322*, 620.
- (12) Goloshchapov, M.; Martynenko, B. *Russ. J. Inorg. Chem. (Engl. Transl.)* **1976**, *21*, 742.

- (13) Cliff, G.; Lorimer, G. W. *J. Microsc. (Oxford)*. **1975**, *103*, 207.
- (14) Visser, J. W. *J. Appl. Crystallogr.* **1969**, *2*, 380.
- (15) De Wolff, P. A. *J. Appl. Crystallogr.* **1968**, *1*, 108.
- (16) Young, R. A.; Wiles, D. B. *J. Appl. Crystallogr.* **1982**, *15*, 430.

Figure 1. TGA curve for MnPO<sub>4</sub>·H<sub>2</sub>O.Table I. Final Profile and Structural Parameters for MnPO<sub>4</sub>·H<sub>2</sub>O

Half-Width Parameters <sup>a</sup> (0.001°)						
$U = 27688$	$(652)$	$V = -11857$	$(314)$	$W = 1667$	$(40)$	
$X = 49$	$(2)$	$Y = 5.5$	$(4)$			
zero-point (0.001°) = 25.09 (10)						
Cell Constants						
$a = 6.912$	$(1)$ Å	$b = 7.470$	$(1)$ Å	$c = 7.357$	$(1)$ Å	
$\beta = 112.3$	$(1)$ °	$V = 351.4$	$(1)$ Å <sup>3</sup>			
tot. no. of allowed reflns: 135						
R Factors (%)						
$R_1 = 4.74$		$R_p = 12.2$		$R_{wp} = 16.1$		
$R_{\text{exptd}} = 15.4$		$\chi^2 = 1.1$				
Structural Parameters						
atom	symm position	x	y	z	B, Å <sup>2</sup>	
Mn(1)	4c	0.2500	0.2500	0.0000		
P(1)	4e	0.0000	0.4176 (2)	0.2500		
O(1)	8f	0.4588 (3)	0.2014 (3)	-0.0995 (3)	0.42 (6)	
O(2)	8f	0.3072 (4)	-0.0359 (3)	-0.3473 (4)	0.34 (6)	
O(3)	4e	0.0000	-0.0995 (5)	0.2500	0.49 (9)	
H(1)	8f	0.075 (6)	-0.014 (4)	0.197 (6)	1.00	
Anisotropic Thermal Parameters <sup>b</sup>						
atom	B(11)	B(22)	B(33)	B(12)	B(13)	B(23)
Mn(1)	0.73 (4)	0.65 (5)	0.27 (5)	0.18 (5)	0.20 (4)	0.08 (4)
P(1)	1.09 (10)	0.48 (10)	0.75 (9)	0.00	0.50 (8)	0.00

<sup>a</sup>The two full width at half-maximum (fwhm) functions are as follows: Gaussian fwhm =  $(U \tan^2 \theta + V \tan \theta + W)^{1/2}$ ; Lorentzian fwhm =  $X \tan \theta + Y/\cos \theta$ . <sup>b</sup>The B's are defined by the general temperature factor expression  $\exp[-1/4(B_{11}h^2a^{*2} + \dots + 2B_{23}k^2l^2c^*)]$ .

The profile analysis used a modified version of the standard Rietveld/Hewat<sup>3,17</sup> program.<sup>18</sup> In this case the peak shape is described by a Voigt function,<sup>16</sup> which is a convolution of Gaussian and Lorentzian components. Refinement of 32 profile and structural parameters, including anisotropic thermal parameters for Mn(1) and P(1), converged to a weighted profile R factor of 16.9% ( $R_1 = 6.3\%$ ). At this stage the assignment of O(3) as a water molecule oxygen was made on the basis of bond length–bond strength calculations.<sup>19</sup> The total valence sum around O(3) due to the two Mn(1) atoms is 0.52, a value typically associated with the presence of two hydrogen atoms. Thus, H(1) was placed geometrically around O(3)—assuming a tetrahedral H–O–H angle of 109.47° and an O–H bond length of 0.9 Å. Subsequent profile refinement (35 parameters, including unrestrained H atom positional parameters, isotropic thermal parameters for the O atoms and anisotropic thermal parameters for Mn(1) and P(1)), converged to final agreement

(17) Hewat, A. W. U.K. At. Energy Auth., Res. Group, Rep. 1973, RRL73/897.

(18) Cox, D. E. *Acta Crystallogr., Sect. A: Found. Crystallogr.* 1984, A40, 369.

(19) Brown, I. D.; Shannon, R. D. *Acta Crystallogr., Sect. A: Cryst. Phys., Diffraction, Theor. Gen. Crystallogr.* 1973, A29, 266.

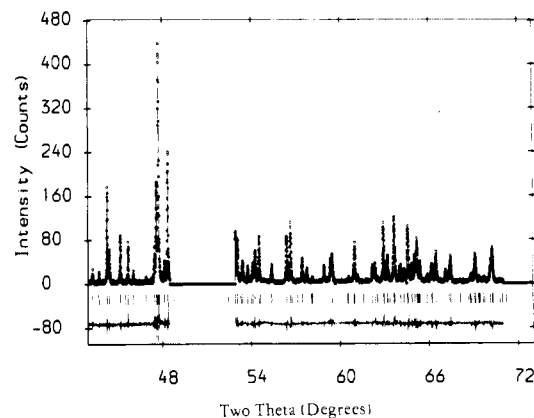
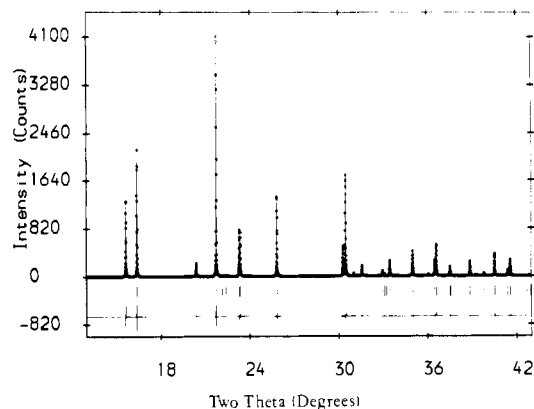


Figure 2. Final observed (open circles), calculated (solid lines), and difference (below) profiles for the Rietveld refinement. Note that the intensity scale is different for the high-angle range. The region between 49 and 53° 2θ is missing due to a malfunction.

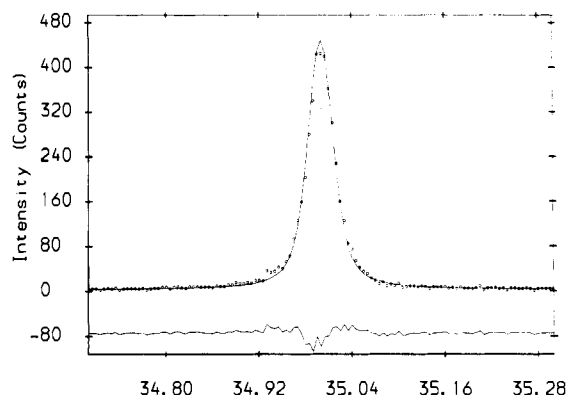


Figure 3. Plot of the observed (open circles), calculated (solid line) and difference (below) profiles for the final fit to the 311 peak, demonstrating the accuracy of the Voigtian description of the peak shape.

factors  $R_{wp} = 16.1\%$ ,  $R_p = 12.2\%$ ,  $R_1 = 4.7\%$ . The function minimized during the refinement was

$$M = \sum_i w_i [y_i(\text{obsd}) - C y_i(\text{calcd})]^2$$

where  $y_i(\text{obsd})$  is the observed intensity at the  $i$ th profile point, after background subtraction,  $C$  is a scale factor and  $y_i(\text{calcd})$  is the calculated intensity at the  $i$ th profile point. Weights are calculated for each profile point from

$$W_i = [(y_i + b_i) + \sigma^2(b_i)]^{-1}$$

where  $b_i$  is the estimated background at the  $i$ th profile point and  $\sigma^2(b_i)$  is the variance of  $b_i$ .

At this stage in the refinement it became apparent that the previously proposed stoichiometry for this phase, MnPO<sub>4</sub>·1.5H<sub>2</sub>O, must be erroneous. A difference Fourier revealed no peaks higher than  $1 \text{ e } \text{Å}^{-3}$ , and furthermore, there appears to be no vacant space in the structure to accommodate the missing 0.5H<sub>2</sub>O. The formula that we arrive at is

**Table II.** Selected Bond Distances (Å) and Angles (deg)<sup>a</sup>

Mn(1)–O(1) × 2	1.886 (3)	P(1)–O(1) × 2	1.529 (4)
Mn(1)–O(2) × 2	1.909 (3)	P(1)–O(2) × 2	1.532 (4)
Mn(1)–O(3) × 2	2.284 (3)	O(2)–O(3) × 2	2.683 (5)
O(1)–Mn(1)–O(1)	180	O(3)–H(1) × 2	1.00 (4)
O(1)–Mn(1)–O(2)	87.8	O(2)–H(1)	1.79 (5)
O(1)–Mn(1)–O(3)	92.9	O(1)–P(1)–O(1)	108.9
O(2)–Mn(1)–O(2)	180	O(1)–P(1)–O(2)	107.8
O(2)–Mn(1)–O(3)	89.1	O(1)–P(1)–O(2)	111.3
Mn(1)–O(1)–P(1)	141	O(2)–P(1)–O(2)	109.7
Mn(1)–O(2)–P(1)	135	O(3)–H(1)–O(2)	148
Mn(1)–O(3)–Mn(1)	121	H(1)–O(3)–H(1)	100

<sup>a</sup>The esd's on the bond angles around Mn, P, O, and H are 0.5, 0.5, 1.0, and 5.0°, respectively.

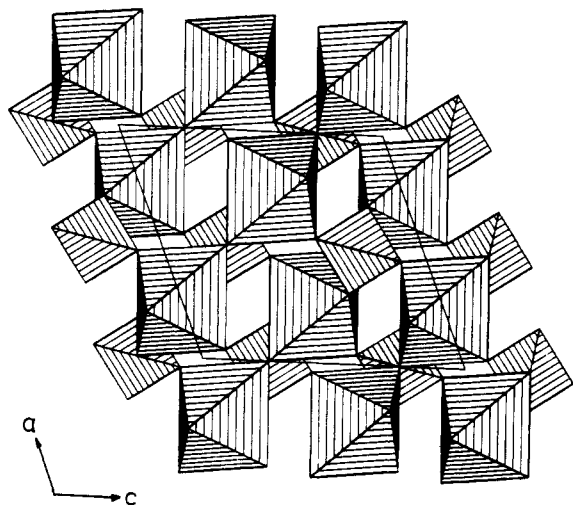


**Figure 4.** STRUPL084 representation of the structure along *b*, showing the direction of the Mn–O–Mn chains. Hydrogen atoms not shown.

therefore  $\text{MnPO}_4 \cdot \text{H}_2\text{O}$ . This is in agreement with the TGA measurements, which may be interpreted as follows:



The calculated weight loss for this transformation is 15.49%, in excellent agreement with the observed value of 15.3%.

## Results

Results of the refinement are given in Table I, and the final observed, calculated, and difference profiles are given in Figure 2. The observed peak shapes are well described by the Voigt function, a typical fit being shown in Figure 3. The relatively large *R* factors are in part due to the falloff of the X-ray form factor at high angle and also to the fact that up to five half-widths need to be taken into account on each side of the peak in order to fit the Lorentzian component. This results in a significant amount of low-intensity data being included in the refinement. A more reliable measure of the quality of the refinement is the "goodness-of-fit" index ( $\chi^2 = (R_{wp}/R_E)^2$ ). The values in Table I demonstrate this.

Final bond distances and angles are given in Table II. The structure consists of a network of  $\text{MnO}_6$  octahedra and  $\text{PO}_4$  tetrahedra linked together by vertex sharing into a continuous three-dimensional array. Trans –Mn–O–Mn– chains run parallel to the 101 direction, the oxygen atom of the water molecule being at the vertex of two adjacent  $\text{MnO}_6$  octahedra. A STRUPL084<sup>20</sup> representation of this is shown in Figure 4. These chains are interconnected by  $\text{PO}_4$  groups such that the resulting framework encloses small channels running parallel to the *c* axis, into which the H atoms of the water molecules project (Figure 5). The  $\text{PO}_4$  tetrahedron is almost regular, whereas the  $\text{MnO}_6$  octahedron shows a considerable tetragonal distortion. The high-spin Mn(III) ion

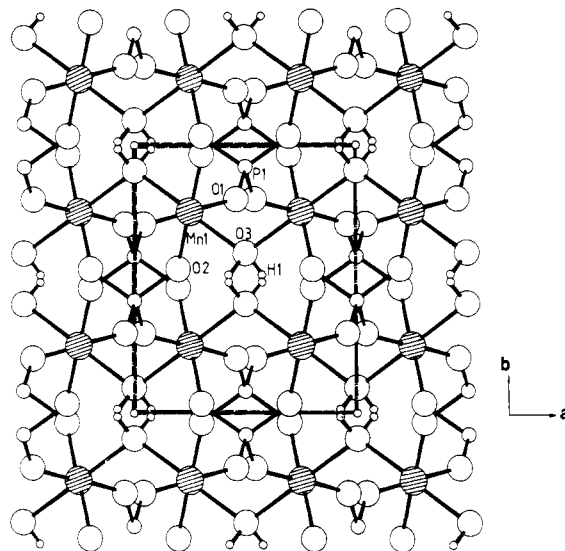


**Figure 5.** Projection of the structure along *c*.

has a  $t_{2g}^3 e_g^1$  electronic configuration and hence is expected to show a Jahn–Teller distortion. The observed bond distances of 1.89, 1.91, and 2.28 Å are similar to those in other manganese(III) oxide systems, e.g.  $\text{NaMnO}_2$ ,<sup>21</sup> which has  $4 \times 1.92$  Å and  $2 \times 2.40$  Å, and  $\text{Mn}_2\text{O}_3$ ,<sup>22</sup> having  $2 \times 2.24$  Å and  $4 \times 1.90$  Å. The hydrogen atom H(1) participates in hydrogen bonding, with O(2) acting as an acceptor at a distance  $\text{H}(1) \cdots \text{O}(2) = 1.79$  Å;  $\text{O}(2) \cdots \text{O}(3) = 2.683$  Å.

A literature search revealed no other phosphates proven to have this stoichiometry. However, the sulfates  $\text{M}^{\text{II}}\text{SO}_4 \cdot \text{H}_2\text{O}$  ( $\text{M}^{\text{II}} = \text{Mn, Fe, Co, Ni, Zn, Mg}$ ) are known and adopt a structure which is very similar to that of  $\text{MnPO}_4 \cdot \text{H}_2\text{O}$ ,<sup>23</sup> but without the Jahn–Teller distortion around the cation. It is interesting to note, however, that  $\text{CuSO}_4 \cdot \text{H}_2\text{O}$ , which may be expected to be truly isomorphous with the present compound due to the requirements of the  $\text{Cu}^{2+}$  ion for a Jahn–Teller distortion, in fact adopts a triclinic rather than monoclinic structure.<sup>24</sup> Thus, in this sense,  $\text{MnPO}_4 \cdot \text{H}_2\text{O}$  may be regarded as unique. For only one of the above compounds has a full single-crystal study been carried out. Bregeault et al.<sup>25</sup> determined the structure of Kieselite,  $\text{MgSiO}_4 \cdot \text{H}_2\text{O}$  including refinement of the hydrogen atom position. In the present case too the H atom can be refined freely, and causes an improvement of 0.8% in  $R_{wp}$ .

## Discussion

We have demonstrated the applicability of high-resolution and high-intensity synchrotron X-ray powder diffraction to two problems in structural solid-state chemistry: (i) the indexing of unknown phases and (ii) the ab initio solution and refinement of relatively simple structures from powder data. The high resolution available on the X13A instrument allows us not only to obtain very reliable indexing for a pure, previously unindexed phase but also to overcome the problem of peak overlap sufficiently to obtain a significant number of integrated intensities for structure solution. We believe that instrumentation is now sufficiently advanced, in both X-ray and neutron powder diffraction, to allow structure determination of simple structures to become relatively routine. Christensen et al.<sup>26</sup> have recently proposed that structures with up to 20 atoms in the asymmetric unit cell could be solved in this

- (21) Jansen, M.; Hoppe, R. *Z. Anorg. Allg. Chem.* **1973**, *399*, 163.
- (22) Geller, S. *Acta Crystallogr., Sect. B: Struct. Crystallogr. Cryst. Chem.* **1971**, *B27*, 821.
- (23) Le Fur, Y.; Coing-Boyat, J.; Bassi, G. *C. R. Seances Acad. Sci., Ser. C* **1966**, *262*, 632.
- (24) Pistorius, C. W. F. T. *Acta Crystallogr.* **1961**, *14*, 534.
- (25) Bregeault, J.-M.; Herpin, P.; Manoli, J.-M.; Pannetier, G. *Bull. Soc. Chim. Fr.* **1970**, 4243.
- (26) Christensen, A. N.; Lehmann, M. S.; Nielsen, M. *Aust. J. Phys.* **1985**, *38*, 497.

(20) Fischer, R. X. *J. Appl. Crystallogr.* **1985**, *18*, 258.

manner. However, we believe this to be a rather conservative estimate, since the limiting factor should be in the refinement rather than solution, once a reliable starting model has been obtained. Indeed, Rudolf et al.<sup>27</sup> have recently solved the structure of an aluminophosphate molecular sieve containing 24 unique atoms, by direct methods.

The present example demonstrates the quality of refinement that may be obtained from synchrotron X-ray data for a pure, well-crystalline phase. The most impressive demonstration of this is the unconstrained refinement of the H atom position. The sensitivity of the refinement to the inclusion of the hydrogen atom probably stems from the fact that manganese occupies a special position and only contributes to 63 ( $hkl$ ,  $k + l = 2n$ ) out of a total of 135 reflections. For the remaining reflections the proportion of scattering due to hydrogen will be relatively high. However, our experience with other data sets suggests that in general major

problems can arise in the refinement of X-ray data. Difficulties arise in adequately describing the X-ray peak shape, particularly when sample-related effects such as anisotropic particle size broadening become important. Future work will probably involve a combination of X-ray and neutron studies. X-ray diffraction is well suited to structure solution, particularly when heavy atoms are present, and neutron diffraction is more appropriate for refinement, due to the more predictable peak shapes.

**Acknowledgment.** A part of this research was carried out at the National Synchrotron Light Source, Brookhaven National Laboratory, which is supported by the Division of Materials Sciences and Division of Chemical Sciences, U.S. Department of Energy. In addition, we would like to thank D. E. Cox for experimental assistance and C. C. Torardi and J. B. Parise for assistance with local computer programs. P. L. would like to thank the SERC for provision of a Research Studentship and Du Pont for hospitality and support during a visit to the Experimental Station.

Registry No.  $\text{MnPO}_4 \cdot \text{H}_2\text{O}$ , 13446-43-0.

(27) Rudolf, P. R.; Saldarriaga-Molina, C.; Clearfield, A. *J. Phys. Chem.* 1986, 90, 6122.

Contribution from the Department of Hydrocarbon Chemistry and Division of Molecular Engineering, Faculty of Engineering, and Faculty of Pharmaceutical Sciences, Kyoto University, Kyoto 606, Japan

## Structure and Oligomerization of Tetrakis(dithioheptanoato)diplatinum

Takashi Kawamura,\*<sup>1a,b</sup> Tsuyoshi Ogawa,<sup>1b</sup> Tokio Yamabe,<sup>1a,b</sup> Hideki Masuda,<sup>1c</sup> and Tooru Taga\*<sup>1c</sup>

Received March 27, 1987

The dinuclear complex  $\text{Pt}_2(n\text{-C}_6\text{H}_{13}\text{CS}_2)_4$  has been prepared from  $\text{K}_2\text{PtCl}_4$  and  $n\text{-C}_6\text{H}_{13}\text{CS}_2\text{H}$ . The crystal of the diplatinum complex is monoclinic, space group  $C2/c$ , with cell dimensions  $a = 36.043$  (10) Å,  $b = 6.079$  (1) Å,  $c = 17.910$  (3) Å,  $\beta = 92.49$  (2)°, and  $Z = 4$ . The structure consists of dinuclear units, with four bridging dithioheptanoato ligands, stacking on the crystallographic 2-fold axis with linear arrangement of Pt atoms. The intra- and intermolecular Pt-Pt distances are 2.855 and 3.224 Å, respectively. Its solution shows thermochromism (brown at room temperature and blue-green at lower temperatures) due to reversible dimerization and further oligomerization. The dimer shows a low-energy absorption at 460 nm, and further self-association induces an absorption at 595 nm, which is comparable with a 620-nm band in the reflectance spectrum of crystalline solids. Thermodynamic data of  $\Delta H = -13$  kcal/mol and  $\Delta S = -41$  cal/(mol K) have been obtained for the dimerization in toluene.

### Introduction

Dinuclear complexes of Pt(II) such as  $\text{Pt}_2(\text{CH}_3\text{CS}_2)_4^2$  and  $\text{K}_4\text{Pt}_2(\text{H}_2\text{P}_2\text{O}_5)_4^3$  are of interest because of an intramolecular partial Pt(II)-Pt(II) bonding interaction arising from 5d-6p mixing<sup>4</sup> and because of the one-dimensional stack in the crystalline state. In the linear stack of  $\text{Pt}_2(\text{RCS}_2)_4$  the intermolecular Pt-Pt distances are short enough (3.08-3.8 Å)<sup>2,5</sup> to produce unusual optical properties. The driving force to form their columnar structures has been suggested to originate from packing of the molecule in the crystalline space rather than intermolecular electronic metal-metal or metal-ligand interactions.<sup>2</sup>

The solubility of  $\text{Pt}_2(\text{CH}_3\text{CS}_2)_4$  is not sufficient to investigate its properties in solution.<sup>2</sup> Tetrakis(dithio-2-methylpropanoato)diplatinum<sup>5</sup> has been reported to have some solubility in toluene, but its behavior in solution has not been explored. To investigate the molecular properties of this class of Pt(II)-Pt(II) d<sup>8</sup>-d<sup>8</sup> systems, we have prepared tetrakis(dithioheptanoato)diplatinum, which has high solubility in organic solvents. The present paper reports the single-crystal X-ray determination of its structure and its reversible oligomerization in solution.

### Experimental Section

Elemental analyses were performed by the Elemental Analysis Center, Kyoto University. Solvents were degassed by flushing with Ar for ca.

20 min when necessary. All reactions and measurements were carried out under Ar.

**Spectroscopy.** Electronic absorption spectra were recorded on a Hitachi 330 spectrophotometer. An Oxford DN1704 variable-temperature liquid-nitrogen cryostat was used to obtain spectra at temperatures below 0 °C. A Hitachi SPR-7 temperature controller was used to observe spectra at temperatures between 0 and 30 °C. Concentrations of solutions for measurements of electronic spectra were corrected for temperature-dependent volume changes by using the thermal expansion data of the pure solvent.<sup>6</sup> Reflectance spectra were observed by using a Hitachi U-3400 spectrophotometer. Vibrational spectra were measured on a Nicolet 20DXB FTIR spectrometer. A Nicolet NT-300 NMR spectrometer was used to obtain <sup>1</sup>H NMR spectra.

**Reagents.**  $\text{K}_2\text{PtCl}_4$ , *n*-hexyl bromide, carbon disulfide, piperidine, and toluene-*d*<sub>8</sub> were obtained from Nakarai Chemicals. THF was distilled from sodium benzophenone ketyl under an Ar atmosphere prior to use. Toluene, *n*-hexane, and dichloromethane were distilled from calcium hydride before use.

**Preparation of Piperidinium Dithioheptanoate.**<sup>7,8</sup> To a mechanically stirred slurry solution of *n*-hexylmagnesium bromide prepared from 50 g (0.30 mol) of *n*-hexyl bromide and 7.3 g (0.30 mol) of magnesium turnings in 105 mL of THF cooled in an ice bath was added 22 g (0.30 mol) of carbon disulfide dropwise over 2.5 h, keeping the temperature of the reaction mixture below 8 °C. The mixture was stirred overnight in an ice bath. To this mixture was added dropwise 70 mL of ice-cold water flushed with Ar, and the mixture was acidified with dropwise addition of 100 mL of an ice-cold and degassed 6 mol L<sup>-1</sup> HCl aqueous solution. After separation of the organic layer, the aqueous layer was extracted three times with 20 mL each of *n*-hexane and the hexane layer

(1) (a) Department of Hydrocarbon Chemistry. (b) Division of Molecular Engineering. (c) Faculty of Pharmaceutical Sciences.

(2) Bellito, C.; Flamini, A.; Piovesana, O.; Zanazzi, P. F. *Inorg. Chem.* 1980, 19, 3632.

(3) Filomena Dos Remedios Pinto, M. A.; Sadler, P. J.; Neidle, S.; Sanderson, M. R.; Subbiah, A.; Kuroda, R. *J. Chem. Soc., Chem. Commun.* 1980, 13.

(4) Reis, A. H., Jr.; Peterson, S. W. *Inorg. Chem.* 1976, 15, 3186.

(5) Bellito, C.; Dessy, G.; Fares, V.; Flamini, A. *J. Chem. Soc., Chem. Commun.* 1981, 409.

(6) Washburn, E. W., Ed. *International Critical Tables of Numerical Data, Physics, Chemistry and Technology*; NRC: Washington, DC, 1928; Vol. III.

(7) Cf.: Houben, J.; Schultze, K. M. L. *Ber. Dtsch. Chem. Ges.* 1910, 43, 2481.

(8) Cf.: Kato, S.; Mizuta, M. *Bull. Chem. Soc. Jpn.* 1972, 45, 3493.